

## Heat exchange calculation in the intermediate container under electron-beam melting

**Iuriy Tsibriy**

*Post-graduate student  
NTUU "KPI"*

**Heorhiy Grabovskiy**

*D.Sc. in engineering  
GNPK "KIA"*

### Abstract

The model of titanium liquid melt heating in the intermediate container of electron-beam furnace is developed considering its flow. On the basis of the developed mathematical model, a series of numerical experiments was conducted using finite-element method and finite-difference method. The analysis of model parameters effect on the melt temperature field formation was carried out. These researches results may be useful for the further development of electron-beam guns control algorithms.

Key words: ELECTRON-BEAM FURNACE, ELECTRON-BEAM GUN, INTERMEDIATE CONTAINER, TEMPERATURE DISTRIBUTION, TITANIUM MELT, PROGRAM OF HEAT EXCHANGE CALCULATION IN THE AREA UNDER INVESTIGATION

### Introduction

Modern engineering technologies require the use of high quality materials with high specific strength, chemical resistance to aggressive media, heat resistance in a wide temperature range and also with other specific properties. Such materials include alloys based on titanium, tantalum, niobium, molybdenum and others [1]. At present, there are various methods of titanium alloys melting. These

include vacuum-arc, plasma, electroslag and electron-beam melting [1, 2].

Comparing to other technologies, melting of titanium alloys using electron beam technology has some advantages such as high quality of alloy purification from harmful impurities, the absence of strict requirements for chemical composition and physical condition of charge material [2, 3]. However, the electron-beam melting technology requires 2-3 times more costs of electricity for the

titanium mass unit smelting comparing with the vacuum-arc melting [3]. When melting, it is difficult to provide the uniform heating of the molten metal surface in the electron-beam furnace (EBF) intermediate container by electron-beam guns (EBG). Also, there is no EBG automatic control system with intermediate container melt temperature feedback in EBF.

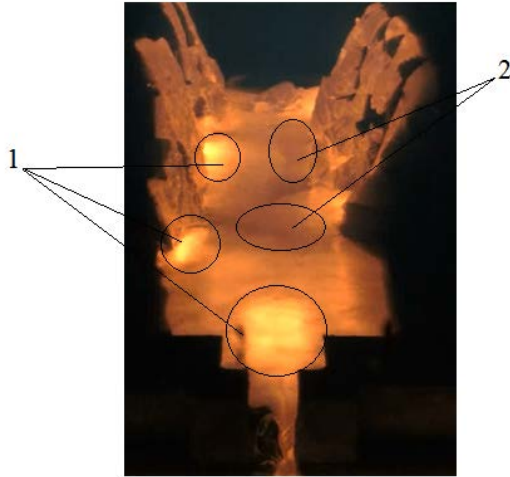


**Figure 1.** Irregularly heated liquid melt in EBG intermediate container:  
- overheated area of melt; 2 – underheated area of melt

The above mentioned disadvantages cause the reduction of EBF efficiency coefficient, the intermediate container central area overheating and its peripheral area underheating (Fig. 1) [4] followed by undesirable changes of the alloy chemical composition [2]. Disadvantages of electron-beam melting can be eliminated through the introduction of EBG control system based on the analysis of the melt thermal condition in the intermediate container.

There are a number of works devoted to the determination of the melt temperature under electron-beam melting. In paper [2], the steady-state heat exchange is considered and the average temperature of the melt volume is calculated. However, this statement does not take into account the temperature change in time as well as non-uniformity of liquid melt temperature fields.

In paper [5], two-dimensional steady-state model of melt heating is suggested. The thermal conductivity is described in cylindrical coordinate system. The temperature fields obtained using the model show melt-ingot transition area. However,

using such model for calculation of heat exchange in the intermediate container, the geometry of the area under investigation and thermal process unsteadiness are not considered.

In papers [6, 7], the three-dimensional unsteady heat exchange models when electron-beam melting are presented. They are used limitedly because they describe unsteady-state heat exchange of liquid melt in the area of beam influence and not in the entire intermediate container, and also they do not consider the process hydrodynamics.

The paper [8] is devoted to determining of the optimal operating conditions of EBG. This model of temperatures calculation is two-dimensional and steady-state considering the melt flow. It describes a heat exchange on the surface of the intermediate container without regard to influence of melt lower layers to the heat exchange and the temperature change in time.

On the basis of analysis, the objective of the research is the development of unsteady-state heat exchange three-dimensional model in the EBF intermediate container considering the melt flow and the analysis of its parameters impact.

Unsteady-state heat exchange model development in the intermediate container

Let us consider thermal and hydrodynamic processes in the intermediate container. The velocity field in the intermediate container initial area is shown in Figure 2. In paper [4], it was found that the melt flow velocity field in EBF FIKO-15M intermediate container is practically homogeneous in the initial area. It is suggested to model the heat exchange process and melt flow under constant flow velocity and straight flow (Fig. 2, marked area) in order to simplify the hydrodynamic problem associated with liquid melt value and flow direction change in the intermediate container. Hereafter, the term "area under investigation" will be understood as the area mentioned above.

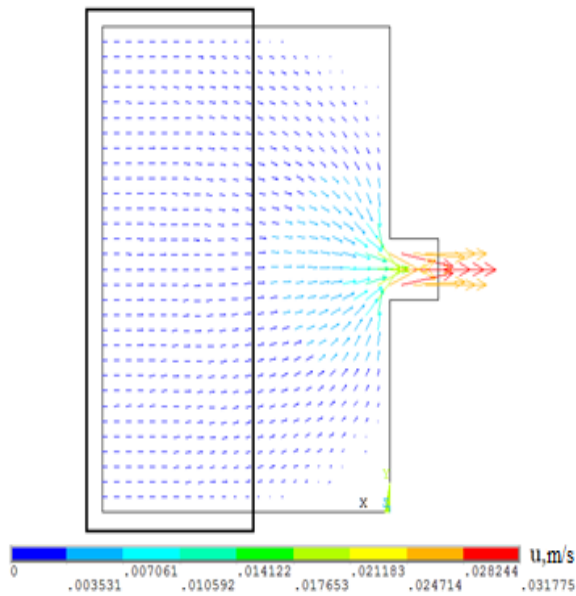


**Figure 2.** The melt flow velocity distribution in the intermediate container marking the modeling area under investigation [4]

Heat exchange in the area under investigation (Fig. 3) may be described by heat conductivity equation considering the melt flow.

$$\frac{\partial T}{\partial t} + u \frac{\partial T}{\partial x} = \frac{\lambda}{c_p \rho} \left( \frac{\partial^2 T}{\partial x^2} + \frac{\partial^2 T}{\partial y^2} + \frac{\partial^2 T}{\partial z^2} \right), (x, y, z) \in V, t > 0, \quad (1)$$

where  $V$  – intermediate container area under investigation;  $x, y, z$  – point position, m;  $t$  – modeling duration time  $t = 80$  s;  $T$  – melt temperature at the point, K;  $u$  – melt flow rate,  $u = 0.003$  m/s;  $\lambda$  – heat conductivity coefficient,  $\lambda = 20$  W/(m·K);  $c_p$  – specific heat capacity at constant pressure,  $c_p = 640$  J/(kg·K);  $\rho$  – melt density,  $\rho = 4120$  kg/m<sup>3</sup>.

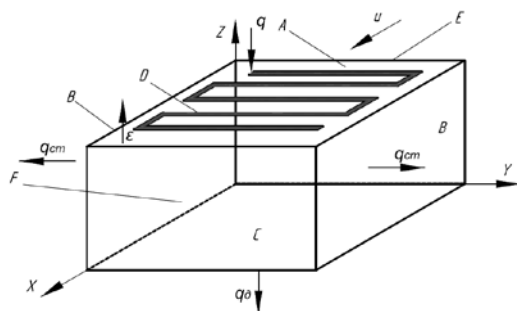


**Figure 3.** Diagram of thermal processes in the area under investigation

It should be noted that the hydrodynamics problem is solved in a simplified form; the flow velocity field is steady and homogeneous. At the initial instant  $t=0$ , the melt temperature in the area under investigation is distributed evenly and is equal to liquid melt melting temperature  $T_0 = 1950$  K:

$$T|_{t=0} = T_0. \quad (2)$$

The boundary conditions in heat exchange: in a predetermined area  $D$  on the surface  $A$  ( $D \subset A$ ) of the area under investigation, the heating is performed by scanning electron beam; the radiation to the environment occurs from the surface  $A \setminus D$ ; the power density extraction  $q_{st} = 0.235 \cdot 10^6$  W/m<sup>2</sup> and  $q_o = 0.15 \cdot 10^6$  W/m<sup>2</sup> is carried out at the bottom through the side faces  $B$  and  $C$  respectively, there is no heat exchange through the input surface  $F$  and  $E$  of melt extraction. These boundary conditions are given below:

$$\left\{ \begin{array}{l} \lambda \frac{\partial T}{\partial z} \Big|_{(x,y,z) \in D} = q_0 \cdot e^{-kr^2}; \\ -\lambda \frac{\partial T}{\partial z} \Big|_{(x,y,z) \in A \setminus D} = \varepsilon \sigma \left( T^4 \Big|_{(x,y,z) \in D} - T_{cep}^4 \right); \\ \lambda \frac{\partial T}{\partial z} \Big|_{(x,y,z) \in C} = q_o; \\ \pm \lambda \frac{\partial T}{\partial y} \Big|_{(x,y,z) \in B} = q_{cm}; \\ \frac{\partial T}{\partial x} \Big|_{(x,y,z) \in E} = \frac{\partial T}{\partial x} \Big|_{(x,y,z) \in F} = 0; \end{array} \right. \quad (3)$$

where  $q_0$  – power density in the center of the focal spot of the beam;  $q_o = 1.5 \cdot 10^6$  W/m<sup>2</sup> [9];  $k$  – concentration coefficient of the electron beam,  $k = 1500$  m<sup>-2</sup>;  $r$  – focal beam radius,  $r = 0.005$  m;  $\varepsilon$  – emissivity factor of titanium melt  $\varepsilon = 0,3$ ;  $\sigma$  – Stefan-Boltzmann constant,  $\sigma = 5,67 \cdot 10^{-8}$  W·m<sup>-2</sup>·K<sup>-4</sup>;  $T_{env}$  – environment temperature,  $T_{env} = 293$  K.

#### Numerical solution of the task

The formulated thermal problem (1) - (3) will be solved with the help of software package Matlab [10] using the method of finite

differences. The implicit splitting scheme on directions [11] is used for heat exchange modeling in the area under investigation. This scheme is that at each time step the three dimensional problems are solved successively along the axis  $X$ ,  $Y$  and  $Z$ . The choice of this scheme is caused by its stability, solving speed and the ability to reduce significantly the computational difficulty of the task.

The program of titanium melt heat exchange calculation in the area under investigation considering its flow was made on the basis of the model and implicit splitting scheme on directions in the software package MatLAB. ANSYS Fluent is widely used for thermal and hydrodynamic processes modeling, and the adequacy of the results has been repeatedly confirmed experimentally [12]. The heat exchange process in the area under investigation considering melt flow at various flow velocities and different heat-transfer coefficients has been modeled in order to test the adequacy of the proposed program in the software package ANSYS Fluent. We have analyzed the character of temperature distribution and their values on the melt surface and also at a depth of 15 mm. It has been noted that the temperature fields obtained using designed program have a similar shape to the temperature fields obtained using the software package ANSYS Fluent, and modeling results error is about 1%.

As an example, the temperature fields obtained using the software package ANSYS Fluent and MatLAB are shown in Fig. 4, 5. The area under investigation dimensions are  $l \times b \times h = 150 \times 400 \times 30$  mm. One electron beam gun performs heating in a predetermined zig-zag path.

As an example, temperature distribution on the melt surface is shown in the Fig. 4 a, b. The range of temperature fields, which is obtained in melt heat exchange calculating program in the area under investigation, corresponds to the range of the modeling results of package ANSYS Fluent. The temperature fields obtained using two methods are compared at a depth of 15 mm in Fig. 5.

In future, we plan to develop an algorithm of EBG beam path control depending on the melt temperature distribution on the intermediate container surface. The heating source coordinates change in the

package ANSYS Fluent modeling process is complex operation and requires writing of additional subprograms which makes it difficult to calculate. Therefore in the future, it was decided to perform modeling in software package MatLAB for EBG control algorithm development because this package provides the ability of control algorithm describing in one program with a description of thermal processes in the area under investigation.

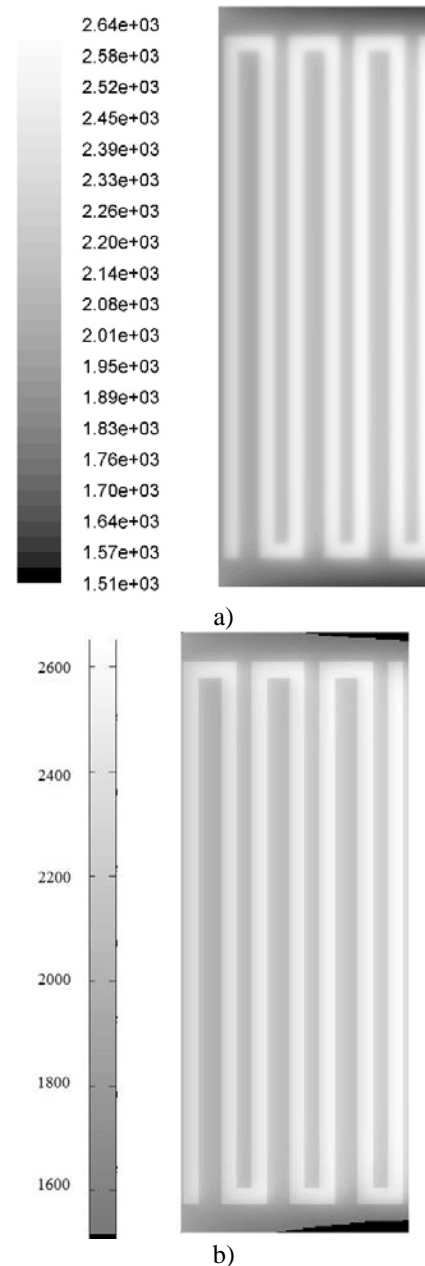
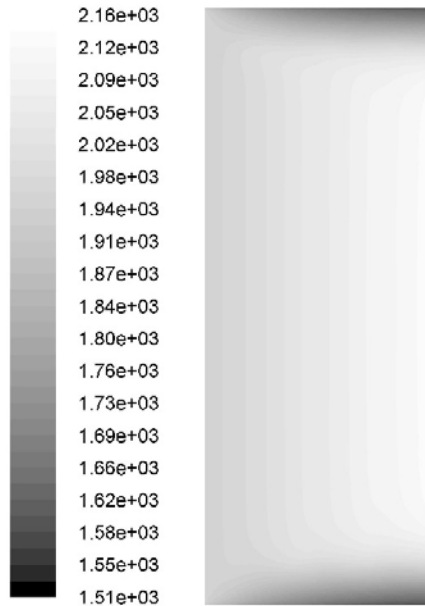


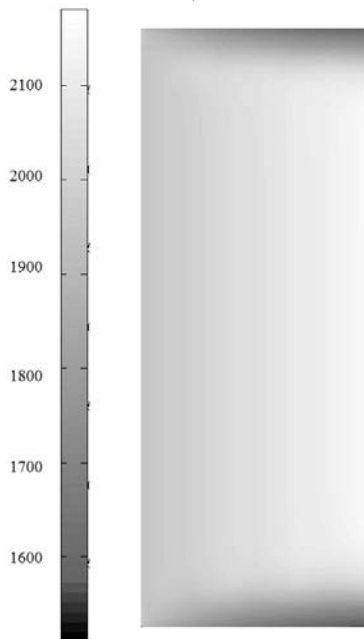
**Figure 4.** Temperature distribution on the melt surface when  $t = 80$  s: a) ANSYS Fluent; b) MatLAB

Also, we performed a modeling of heat exchange in the area under investigation at different parameters values: melt flow rate  $u$ ;

electron beam power density, power density  $q_{st}$  and  $q_o$ , which are extracted through the walls and bottom of the investigated area; the degree of irregularity in the distribution of electron beam capacity on the surface of the investigated area,  $n$ .



a)

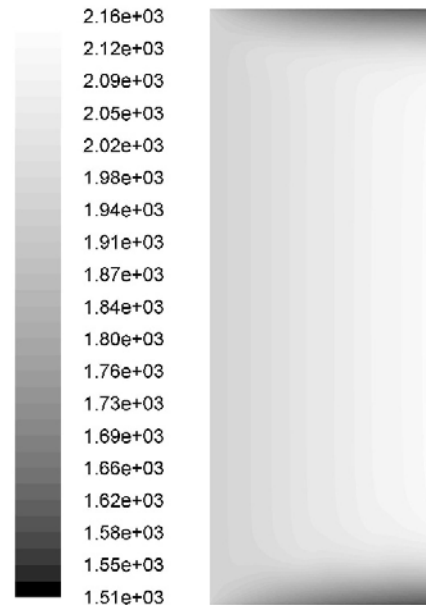


b)

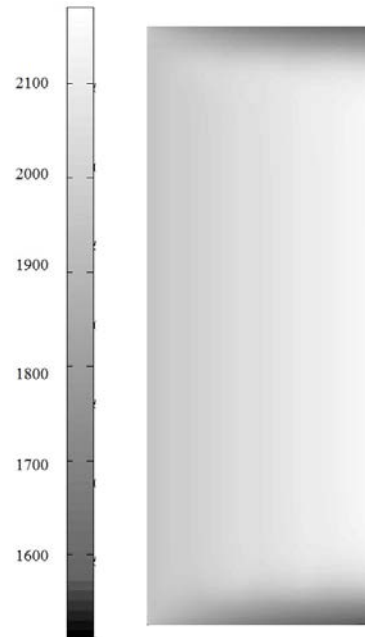
**Figure 4.** Temperature distribution on the melt surface when  $t = 80$  s: a) ANSYS Fluent; b) MatLAB

Also, we performed a modeling of heat exchange in the area under investigation at different parameters values: melt flow rate  $u$ ; electron beam power density, power density  $q_{st}$

and  $q_o$ , which are extracted through the walls and bottom of the investigated area; the degree of irregularity in the distribution of electron beam capacity on the surface of the investigated area,  $n$ .



a)



b)

**Figure 5.** Temperature distribution at the melt depth of 15 mm when  $t = 80$  s: a) ANSYS Fluent; b) MatLAB

### Analysis of the results

*Melt flow rate impact.* The melt temperature distributions on the investigated area surface when various values of  $u$  are shown in Fig. 6. According to the obtained results with an increase of rate, the melt

temperature in the central area is reduced. This comes from the fact that the melt needs more time to be heated by electron beam when flowing. The small values of flow rate  $u$  increase cause the temperature reduction in the peripheral area (Fig. 6 a, b). With further increase of  $u$ , the temperature rises as a result

of reduction of the contact time of the molten metal with cooled walls (Fig. 6 b, c, d).

It should be noted that in the peripheral area, the melt temperature is below the melting point which actually causes crystallization of the liquid metal.

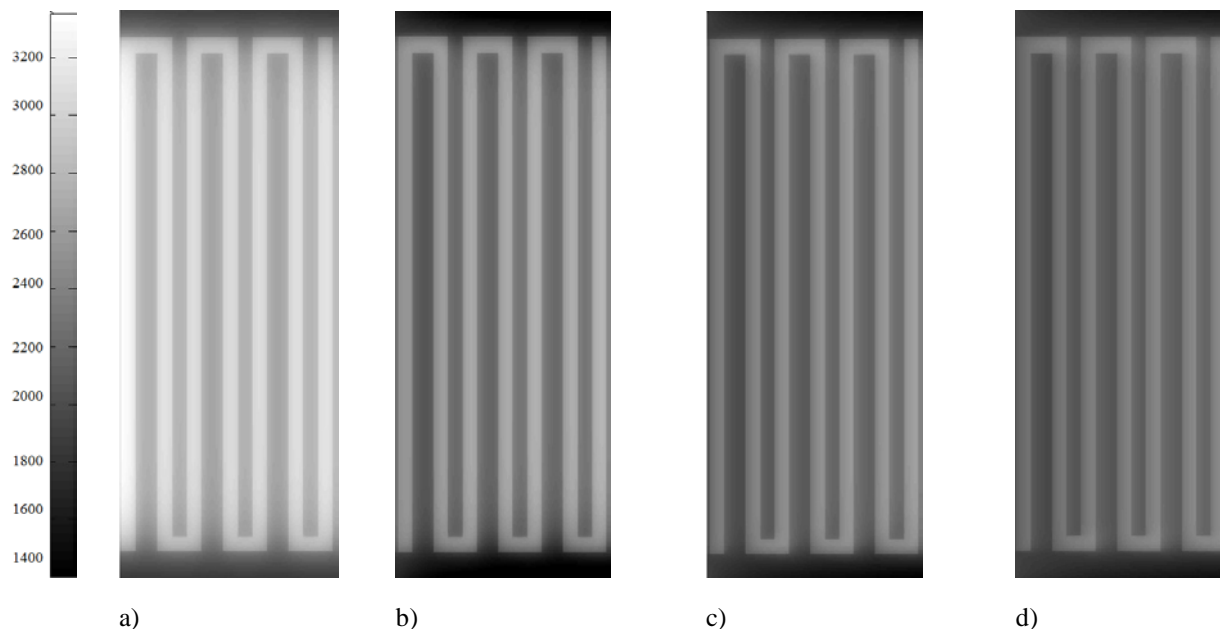


**Figure 6.** Temperature distribution on the melt surface when flow rates if  $t = 80$  s: a)  $u=0$ ; b)  $u=0.001$  m/s; c)  $u=0.003$  m/s; d)  $u=0.006$  m/s

*The electron beam power density impact.* The melt temperature distribution on the surface of the investigated area is obtained for different values of  $q$  and is shown in Figure 7. From this

distribution, it follows that increase in electron beam power density raises the temperature in central area of the investigated area, and the melt temperature change at the peripheral area is not significant.

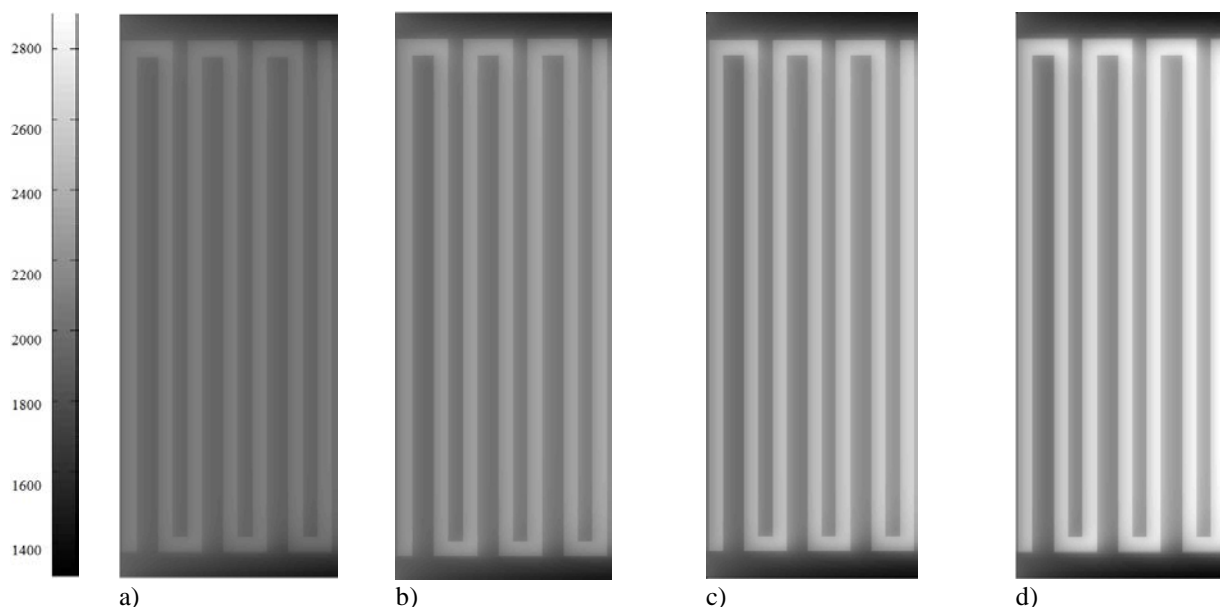
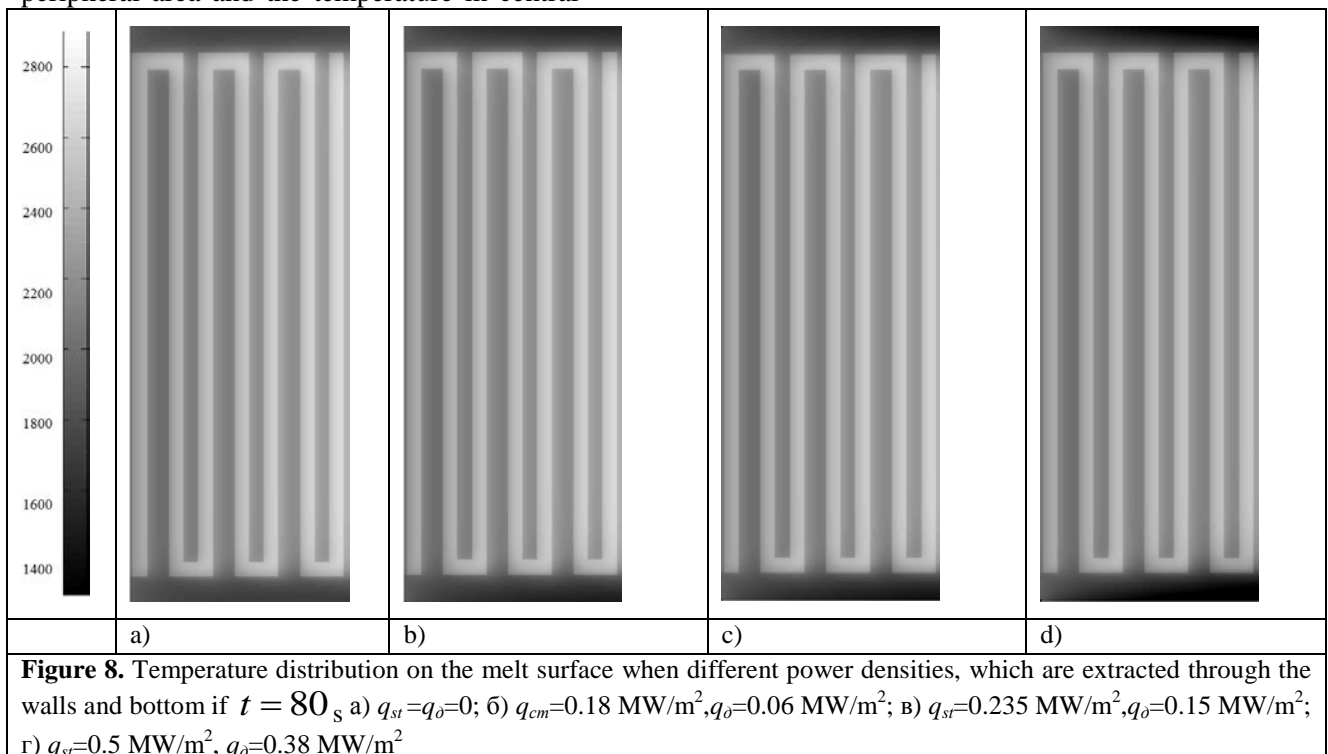


**Figure 7.** Temperature distribution on the melt surface when different heating power densities if  $t = 80$  s: a)  $q=0.5$  MW/m<sup>2</sup>; b)  $q=1$  MW/m<sup>2</sup>; c)  $q=1.5$  MW/m<sup>2</sup>; d)  $q=2$  MW/m<sup>2</sup>

*The investigated area bottom and walls cooling rate impact.* The modeling results of the temperature distribution on the surface of the area under investigation when various power densities, which are extracted through the walls and bottom of investigated area, are shown in Fig. 8. The increase of  $q_{st}$  and  $q_o$  causes the melt temperature in peripheral area and the temperature in central

area reduction. Let us note that the melt temperature on the bottom of investigated area is also reduced. It should be noted that the reduction in melt temperature is insignificant compared to the change in the flow rate and heating power density. The values of  $q_{st}$  and  $q_o$  correspond to the data presented in the paper [2].



*The impact of density distribution irregularity of electron beam on the investigated area surface.* The surface of investigated area was divided into two equal parts perpendicularly to the flow. We

performed the modeling for various electron beam path, wherein the left part is fed with  $n$  % of the total brake power and the right one is fed with  $100\% - n$  % respectively.

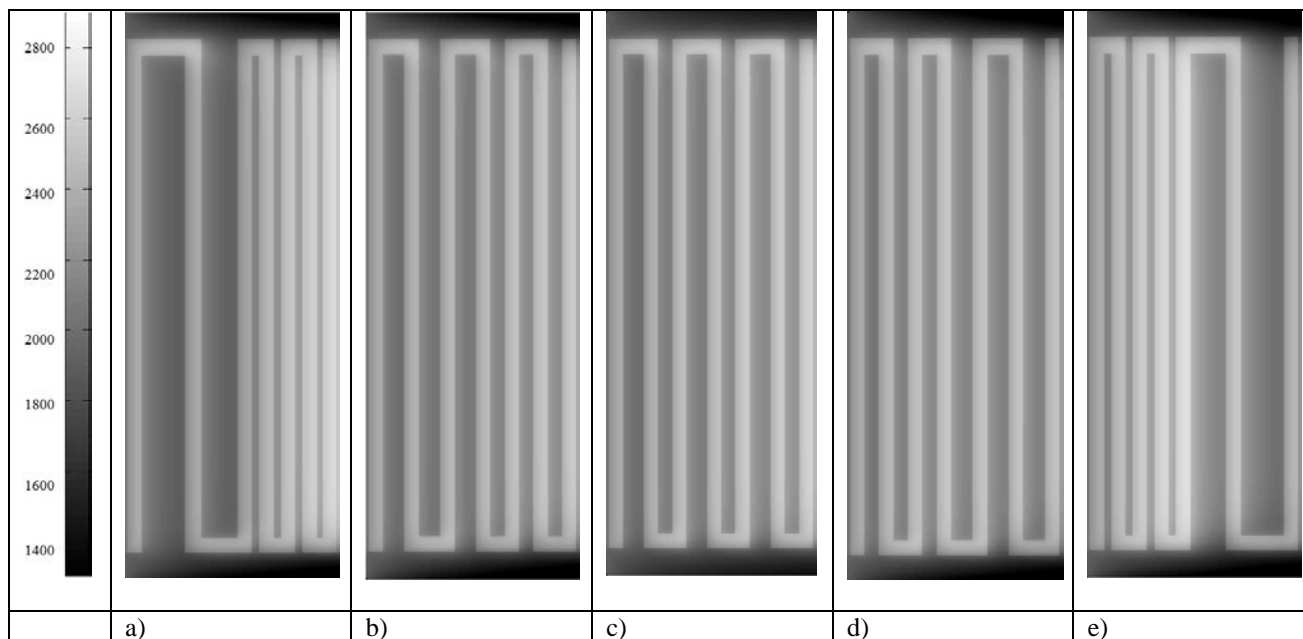


**Figure 9.** Temperature distribution on the melt surface when  $t = 80$  s a)  $n = 30\%$ ; b)  $n = 43\%$ ; c)  $n = 50\%$ ; d)  $n = 57\%$ ; e)  $n = 70\%$

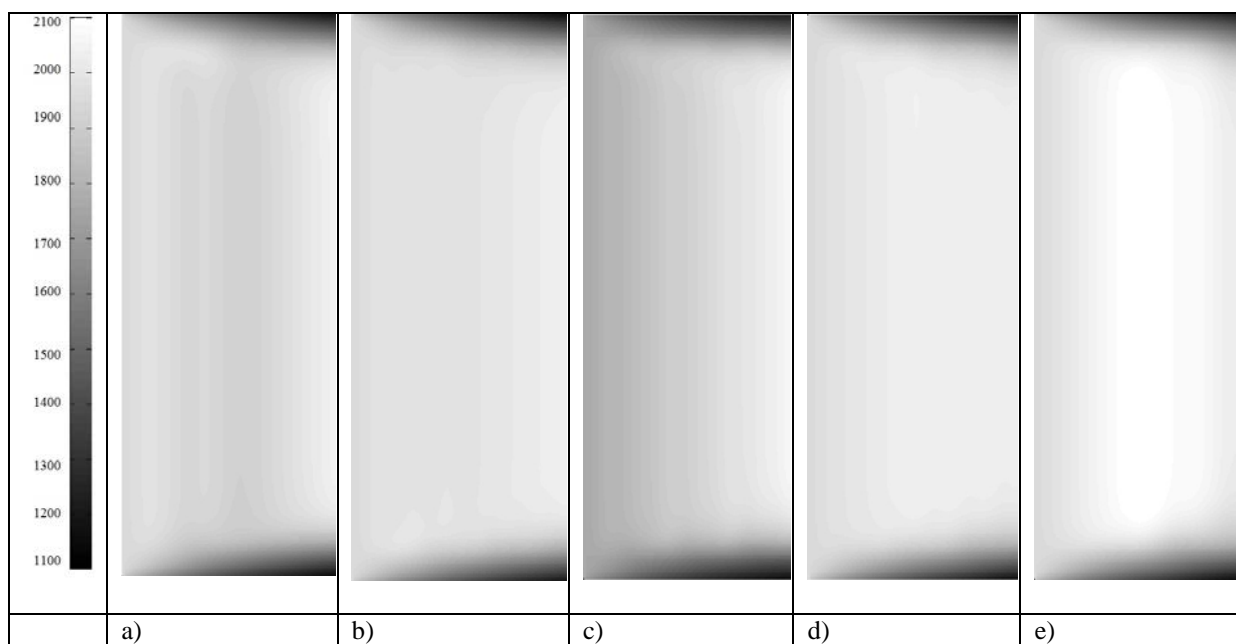


**Figure 10.** Temperature distribution in the melt investigated area at the depth of 15 mm when  $t = 80$  s: a)  $n = 30\%$ ; b)  $n = 43\%$ ; c)  $n = 50\%$ ; d)  $n = 57\%$ ; e)  $n = 70\%$

The temperature fields analysis shows that the melt is heated not enough at the depth of 15 mm when low-grade heating of the left part. Its temperature is close to the phase transition temperature which is undesirable (Fig. 9 a, b, 10 a, b). Also if  $n = 30\%$ , the right part is overheated on the surface (Fig. 9 a). When heating power uniform distribution (Fig. 9 c, 10 c), the melt is heated to the required temperature, but the melt surface on

the right side may be overheated. The temperature distribution is not uniform at the depth of 15 mm when  $n = 50\%$ . When moderate overheating of the left part (Fig. 9 d, 10 d), the melt is heated uniformly at the depth and is of permissible temperature on the surface. When significant overheating of the left part, the melt is overheated on the surface and the temperature distribution at the depth is not uniform (Fig. 9 e, 10 e).



Thus, there is a range of optimum ratios of the EBG power distribution on the melt surface, wherein the uniform heating occurs throughout the volume and is in the range  $n = 55 - 60\%$ .

### Conclusions

The model of titanium liquid melt unsteady-state heating in EBF investigated area is shown considering its flow. The model is implemented using the finite-difference method. The modeling is performed on the basis of selected numerical method.

We performed the modeling of titanium liquid melt unsteady-state heating in the area under investigation at different flow velocities, heating power densities, cooling power densities of the walls and bottom, and also at various heating power distributions on the surface of investigated area.

According to the modeling results, we have found:

The melt flow rate increasing causes the temperature reduction in the central area of investigated area and insignificant increase in the melt temperature in the area of its contact with the walls and the bottom of investigated area;

Increase in heating power density raises the temperature of the central area to impermissible values, and the melt temperature in the peripheral area is hardly changed;

Changing of cooling intensity of the walls and bottom of investigated area reduces the melt temperature in a peripheral area while the temperature change is insignificant in the central area;

For melt uniform heating throughout the volume of intermediate container to temperatures above the melting point, it is desirable to heat its surface at the flow initial part by 5-10% more than the part of the further flow.

### References

1. Paton B.E. *Elektronno-luchevaya plavka tugoplavkikh i vysokoreaktsionnykh metallov*. [Electron-beam melting of refractory and high-reactive metals]. Kyiv, Naukova dumka, 2008, 312 p.
2. Paton B.E., Trigub N.P., Akhonin S.V., Zhuk G.V. *Elektronno-luchevaya plavka titana*. [Electron-beam melting of titan]. Kyiv, Naukova dumka, 2006, 248 p.
3. Minakova A.B., Minakov V.N., Minakov N.V., Trefilov V.I. *O strukture proizvodstva titanovoy produktsii: mirovoy opyt i realizatsiya v Ukraine*. [The production structure of titanium products: the world experience and implementation in Ukraine]. Kiev, IPMS, 1998, 22 p.
4. Tsibriy Yu.O. (2014) Modelling of temperature distribution of molten titanium considering its flow. *Journal of NTUU "KPI", series "Mashinobuduvannya"*, No72, p.p. 65-71.
5. Vutova K. (1999) Computer simulation of the heat transfer during electron beam melting and refining. *Vacuum*. No53, p.p. 87-91.
6. Cline H. E. (1977) Heat treating and melting material with a scanning laser or electron beam. *Journal of Applied Physics*. No48, p.p. 3895-3900.
7. Markov A.B. (1997) Calculation and experimental determination of dimensions of hardening and tempering zones in quenched U7A steel irradiated with a pulsed electron beam. *Instruments and Methods in Physics Research*. p.p.79-86.
8. Sergienko S. N. *Resursoberegayushchaya tekhnologiya polucheniya slitkov titana na ustanovke elektronno-luchevogo pereplava s promezhutochnoy emkost'yu*. [Resource-saving technology of titanium ingots obtaining on the electron beam melting installation with an intermediate container: the thesis of PhD in Technical Sciences, 05.16.02]. Orsk, 2011, 134 p.
9. Ladokhin S. V., Levitskiy N. I., Chernyavskiy V. B., Lapshuk T. V., Shmigidin V. G., Kravchuk L. A., Gladkov A. S. *Elektronno-luchevaya plavka v liteynom proizvodstve*. [Electron beam melting in foundry manufacture]. Kiev, Stal', 2007, 626 p.
10. Dzhon G. Met'yuz, Kurtis D. Fink *Chislennyye metody. Ispol'zovanie MATLAB*. [Numerical methods. Using of MATLAB. III publ., tran. from English]. Moscov, Vil'yame, 2001.720 p. ISBN 5-8459-0162-6.

11. Yanenko N.N. *Metod drobnykh shagov resheniya mnogomernykh zadach matematicheskoy fiziki.* [Fractional steps method for multivariate problems solving of mathematical physics]. Novosibirsk, Nauka, 1967. 196 p.
12. Karvatskiy A. N. Teploelektrichniy ta mekhanichniy stan

visokotemperaturnikh energoemnikh promislovikh agregativ. [Thermal-conductivity and mechanical condition of high energy-consuming industrial units: the thesis of D.Sc. in engineering,05.05.13]. Kyiv, 2010. 438 p.

